JOURNAL OF MATERIALS SCIENCE 30 (1995) 2785–2792

Protonic and oxygen-ion conduction in $SrZrO_3$-based materials

J.A. LABRINCHA, F.M.B. MARQUES, J.R. FRADE
Departamento de Engenharia Cerâmica e do Vidro, Universidade de Aveiro, P-3800 Aveiro, Portugal

Strontium zirconate-based materials have been studied as potential high-temperature protonic conductors. Yttrium for zirconium substitution, and lanthanum for strontium substitution were selected to demonstrate that changes in composition can be used as a tool to design the properties. At temperatures below about 900° C, both yttrium-doped and undoped strontium zirconate are mostly protonic conductors at oxygen partial pressures below about 1 Pa, and mixed ionic and p-type conductors at higher pressures. The main ionic contribution changes from mostly protonic to oxygen-ion conduction with increasing temperature, which may affect the performance of electrochemical devices. Yttrium for zirconium substitution enhances both the electronic and ionic conductivities. Lanthanum for strontium substitution suppresses protonic conduction and gives rise to mixed oxygen-ion and n-type conduction in reducing conditions.

1. Introduction

Strontium zirconate was first studied for use in MHD generators [1, 2], and as a dielectric material [3]. It has a perovskite-type ABO_3 structure. Strontium substitution by a trivalent cation can be compensated by A-site vacancies [4]. Zborowska *et al.* [5] obtained single-phase $Sr(ZrTi_x)\ O_{3+\delta}$ compositions with up to 5% TiO_2, which also corresponds to a strontium-deficient perovskite. These titania additions were found to enhance the electrical conductivity by a factor of about 10.

Recent interest in $SrZrO_3$-based materials is due to the discovery that some of these materials are high-temperature protonic conductors [6–9]. Protonic conduction was first discovered in $SrCe_{1-x}M_xO_{3-\alpha}$ materials (M = Y, In, Zn, Nd, Sm or Dy) [10], and has now been observed in other materials with the perovskite structure, including materials based on $BaCeO_3$ [11–17], $BaZrO_3$ [9, 16], $CaZrO_3$ [8, 9, 18], etc. Unfortunately, the highest protonic conductivities were found in chemically unstable systems such as $BaThO_3$-based materials [19]. Cerate materials might also fail in CO_2 containing atmospheres [20].

Several experimental techniques were used to study the transport properties of proton-conducting ABO_3-based materials, including hydrogen concentration cells [9, 10, 17], water vapour concentration cells [10, 16, 21–23], hydrogen pumping or steam electrolysis [9, 10, 12, 24], and the ratio between the rates of water vapour release at the cathode and anode of fuel cells [14, 25]. The effects of water vapour and isotope effects on conductivity [9, 10, 15, 23], the dependence of conductivity on the oxygen partial pressure [13, 22, 26], and measurements of proton and oxygen-ion diffusion coefficients [27] were also used for similar purposes. Simultaneous release of water vapour at the anode and at the cathode of fuel cells was used to calculate the oxygen-ion and protonic transport numbers [14, 21, 25], and the change in conductivity for p_{O_2} higher than about 10 Pa has been attributed to electron hole transport [22, 23, 26]. In addition, Bonanos [13] found the onset of an n-type conductivity component for $BaCe_{0.9}Gd_{0.1}O_{3-\alpha}$ in reducing conditions, and Labrincha *et al.* [26] reported that lanthanum for strontium substitution in $SrZrO_3$ also gives rise to the n-type contribution in reducing conditions.

Iwahara *et al.*'s original work [10] showed that the protonic transport number in ABO_3-based protonic conductors drops with increasing temperature. It has now been demonstrated that the protonic transport numbers in some cerate materials drop with increasing temperature, both because of an increasing oxygen-ion contribution, and also due to drop in protonic conductivity for excessively high temperatures [14, 25, 28]. The concentration of protonic charge carriers decreases with increasing temperature and increases with the water vapour partial pressure [25, 28]. In addition, the onset of a p-type contribution for relatively high oxygen partial pressures [22] can also cause a decrease in protonic transport numbers.

The increase in activation energy for the temperature dependence of conductivity [6, 7, 9, 10] also suggests that the dominant charge carrier changes at some intermediate temperature range.

The change from a major protonic transport number to a large oxygen-ion transport number may affect the behaviour of electrochemical devices. For example, this might explain the failure of some electrochemical

0022–2461

sensors [17]. Fuel cells might also be affected if the electrolyte is a mixed oxygen-ion and protonic conductor. Note that the water vapour discharge occurs at the cathode when the electrolyte is a protonic conductor, at the anode for an oxygen-ion conductor, or at both electrodes when the oxygen-ion and protonic conductivities are similar.

Substitution of a trivalent dopant, M, for a tetravalent species, B, is usually needed to achieve protonic conduction in $ACe_{1-x}M_xO_{3-\alpha}$ or $AZr_{1-x}M_xO_{3-\alpha}$ materials [22, 26]. The charge compensation can be provided by oxygen-ion vacancies, protons and/or electron holes [6, 22, 28]. Huang *et al.* [7] found the highest conductivity in $SrZr_{1-x}Y_xO_{3-\alpha}$ for about 5% Y for zirconium substitution, but the conductivity of some cerate materials reaches its maximum for higher additions of heterovalent dopant [25].

In a previous paper [26], we proposed a defect structure for $SrZrO_3$-based materials which accounts for mixed protonic and oxygen-ion conduction. This model explains the effects of oxygen partial pressure on conductivity, and is consistent with the effects of composition. The present work confirms this model and describes the changes from protonic to oxygen-ion conduction on changing temperature and oxygen partial pressure.

2. Experimental procedure

Three $SrZrO_3$-based compositions were prepared and characterized as described elsewhere [26]. The notation SZ, SYZ, and LSZ was used for $SrZrO_3$, $SrZr_{0.84}Y_{0.16}O_{2.92}$, and $Sr_{0.95}La_{0.05}ZrO_{3.025}$. The relative density of the samples was about 63% for SZ, 64% for SYZ and 97% for LSZ. X-ray diffraction was used to confirm that these compositions yield single-phase materials with the perovskite structure.

Impedance spectroscopy was used for characterizing the materials in air, and to select a frequency for a.c. conductivity measurements. A two-probe constant frequency (10 kHz) a.c. method was used to study the effects of oxygen partial pressure on the electrical conductivity, in the temperature range 800–1100 °C. These measurements were performed in a furnace with an oxygen sensor and an electrochemical pump to achieve reducing conditions, as described by Marques and Wirtz [29]. The furnace was flushed by flowing nitrogen to give a nearly constant humidity in the atmosphere, and to bring the oxygen partial pressure down to about 10 Pa. The lower limits of oxygen partial pressures reached by electrochemical pumping were about 10^{-12} Pa at 1100 °C to 10^{-18} Pa at 800 °C. The electrical measurements were then recorded during the reoxidation, for oxygen partial pressures up to about 2×10^4 Pa. The specimens were electroded with porous platinum (Engelhard 6926) for impedance spectroscopy and conductivity measurements.

3. Transport properties

3.1. Impedance spectra

Fig. 1 shows impedance spectra in the range 20–10^6 Hz for the undoped (SZ), yttrium-containing

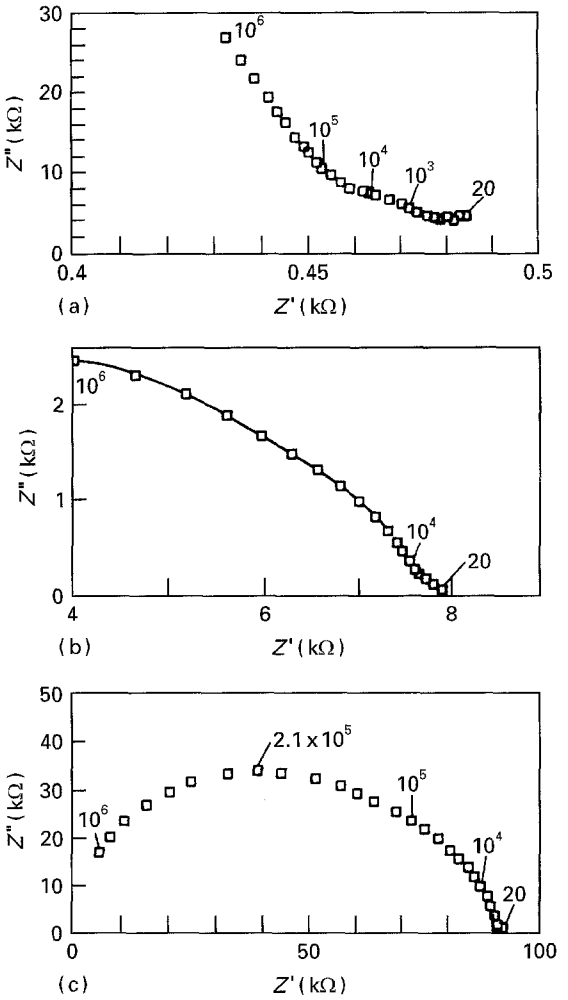

Figure 1 Impedance spectra of (a) $SrZr_{0.84}Y_{0.16}O_{2.92}$ (SYZ), (b) $SrZrO_3$ (SZ), and (c) $Sr_{0.95}La_{0.05}ZrO_{3.025}$ (LSZ) for the frequency range 20–10^6 Hz, in air, and at 800 °C. The numbers show some frequency values.

(SYZ) and lanthanum-containing (LSZ) materials at 800 °C. A parallel RC circuit is often assumed to describe the bulk behaviour of ionic conductors. The impedance spectrum (Z'' versus Z') then becomes a semicircle which is centred at $Z' = R/2$, and $\omega = (RC)^{-1}$ is the relaxation frequency. The relaxation frequency corresponds to the maximum of Z'' versus Z'. The relaxation frequency for the lanthanum-containing sample is about 2×10^5 Hz at 800 °C. At this temperature the estimated relaxation frequency is significantly higher than 10^6 Hz in the undoped sample (SZ), and much higher than 10^6 Hz in the yttrium-containing sample. Differences in relaxation frequencies and the corresponding differences in activation energies are usually understood as a result of different mobile species and/or defect interactions when dealing with similar host lattices.

Impedance spectra can also be used to evaluate the resistance of the sample; this corresponds to the intersection of the arc with the real axis, in the lower frequency range. Fig. 1 thus shows that a typical 10^4 Hz frequency can be used for a.c. conductivity measurements, with errors smaller than 5% at 800 °C or higher temperatures.

The impedance spectra of the LSZ composition shown in Figs 1 and 2 suggests the coexistence of two

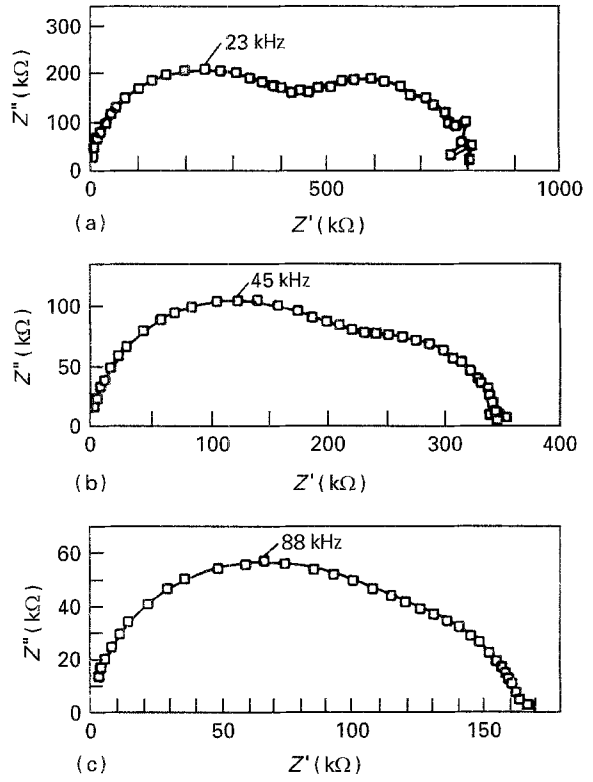

Figure 2 Impedance spectra for $Sr_{0.95}La_{0.05}ZrO_{3.025}$ at (a) 650, (b) 700 and (c) 750 °C.

contributions, rather than a single *RC* equivalent circuit. The high-frequency contribution is believed to correspond to the bulk behaviour of the sample, and the second component is probably due to a resistive grain boundary, as found frequently for solid oxide electrolytes. Fig. 2 shows that the bulk and grain-boundary contributions are similar at about 650 °C, while the grain-boundary term decreases with increasing temperature.

The bulk and grain-boundary components of SZ and SYZ could not be separated for temperatures higher than about 500 °C. In fact, the relaxation frequencies become higher than the upper limit provided by the experimental equipment (10^6 Hz). Nevertheless, the lower frequency limit of bulk or grain-boundary arcs can still be used to evaluate the resistance and compute the conductivity for temperatures up to about 1000 °C (Fig. 3).

3.2. Effects of oxygen partial pressure

Fig. 4 shows the effect of oxygen partial pressure on the a.c. conductivity of undoped $SrZrO_3$. The conductivity is nearly independent of the oxygen partial pressure in the intermediate range; this usually corresponds to ionic conduction in oxide compounds. The increase in conductivity in the high-pressure range (above 10 Pa), is typical of p-type conduction. On the contrary, the drop in conductivity at low oxygen partial pressures is rather unusual. Labrincha *et al.* [26] have shown that this effect can be related to a decrease in protonic conductivity for low oxygen partial pressures. A similar explanation was proposed by Norby *et al.* [30–32] to explain changes in protonic contributions in sesquioxides.

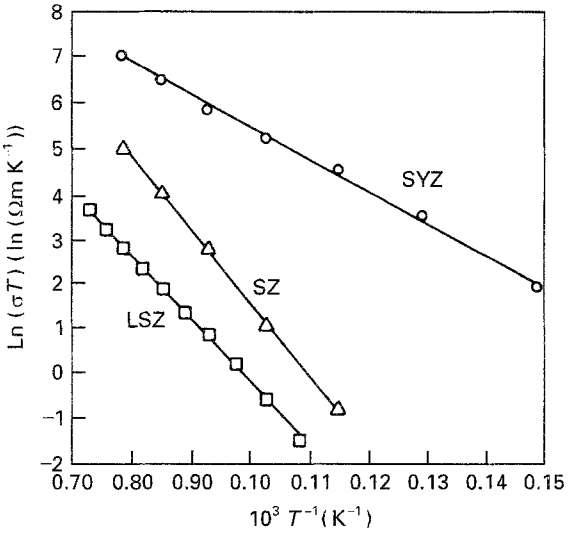

Figure 3 Temperature dependence of conductivity in air for samples with compositions $SrZrO_3$ (SZ), $SrZr_{0.84}Y_{0.16}O_{2.92}$ (SYZ) and $Sr_{0.95}La_{0.05}ZrO_{3.025}$ (LSZ).

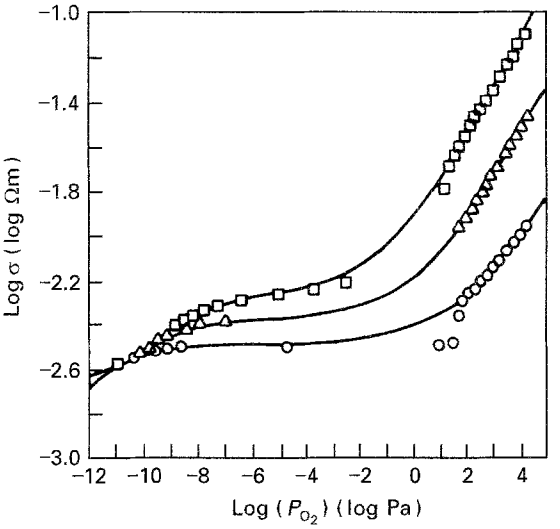

Figure 4 Electrical conductivity of $SrZrO_3$ versus the oxygen partial pressure at (○) 900, (Δ) 1000 and (□) 1100 °C.

According to the literature [6, 22], the incorporation of protons in ABO_3-based perovskite materials can be described by

$$2V_O^{\cdot\cdot} + O_2(g) \rightleftharpoons 2O_O + 4h^{\cdot} \quad (1)$$

$$V_O^{\cdot\cdot} + H_2O(g) \rightleftharpoons 2H_i^{\cdot} + O_O \quad (2)$$

using the Kroger–Vink notation. The model proposed by Labrincha *et al.* [26], includes these reactions and also the effect of variable water vapour to hydrogen ratio expected for the following reaction

$$2H_2O(g) \rightleftharpoons 2H_2(g) + O_2(g) \quad (3)$$

According to this model, the effect of gas composition on the electrical conductivity then becomes

$$\sigma = \sigma_{i1} + \sigma_p^*(p_{O_2})^{1/4} + \sigma_{i2}/(1 + p_{H_2}/p_{H_2O})^{1/2} \quad (4)$$

where p_{O_2}, p_{H_2} and p_{H_2O} are the partial pressures of oxygen, hydrogen and water vapour. The relevant parameters in Equation 4, correspond to the oxygen ion, σ_{i1}, protonic, σ_{i2}, and electronic, σ_p^*, conductivity contributions. The value of σ_{i2} is the protonic

TABLE I Fitting parameters for materials with compositions $SrZrO_3$ (SZ), $SrZr_{0.84}Y_{0.16}O_{2.92}$ (SYZ) and $Sr_{0.95}La_{0.05}ZrO_{3.025}$ (LSZ)

Conductivity	Composition	800 °C	900 °C	1000 °C	1100 °C
σ_{i1} ($10^3\Omega^{-1}$ m^{-1})	SZ	–	0.8	1.4	2.1
	LSZ	2.9	7.2	12.5	20
	SYZ	12	27	62	96
σ_{i2} ($10^3\Omega^{-1}$ m^{-1})	SZ	–	2.4	2.7	3.1
	SYZ	54	48	39	24
σ_p^*($10^3\Omega^{-1}$ m^{-1} Pa$^{-1/4}$)	SZ	–	0.62	2.3	6.5
	SYZ	12.5	25	44	55
σ_n^*($10^6\Omega^{-1}$ m^{-1} Pa$^{1/4}$)	LSZ	0.14	1.8	24	130

conductivity when the hydrogen to water vapour ratio tends to zero, and σ_p^* is the electron hole conductivity when the oxygen partial pressure is 1 Pa.

The hydrogen to water vapour ratio was computed by assuming that Reaction 3 is in equilibrium

$$p_{H_2}/p_{H_2O} = \exp[\Delta G/(2RT)](p_{O_2})^{-1/2} \quad (5)$$

where ΔG is the Gibbs free energy of reaction $2H_2 + O_2 \rightleftharpoons 2H_2O$.

Equations 4 and 5 give reasonably good fitting (full line) for the experimental results as shown in Fig. 4, except for a range of about 10^{-4}–10^{1} Pa. The relevant parameters are shown in Table I. Failure of oxygen sensor readings is believed to account for these deviations [29].

The conductivity data measured for the yttrium-containing samples is also reasonably described by Equations 4 and 5 (Fig. 5). Yttrium for zirconium substitution enhances the conductivity by at least one order of magnitude relative to the undoped material. The largest increase is for the oxygen-ion component, but the protonic and electronic contributions also increase by about one order of magnitude. These effects of yttrium for zirconium substitution have been explained according to the following reaction

$$Y_2O_3 + 2SrO \xrightarrow{SrZrO_3} 2Y'_{Zr} + 2Sr_{Sr} + 5O_O + V_O^{\cdot\cdot} \quad (6)$$

This reaction enhances the concentration of oxygen vacancies and explains the increase in oxygen-ion conductivity (Table I). In addition, combination with Reactions 1 and 2 also predicts enhanced concentrations of protons and electron holes, which explains the increase in the corresponding conductivity components.

The fitting parameters, σ_{i1}, σ_{i2} and σ_p^*, are also useful to compute the changes of transport numbers $t_j = \sigma_j/\sigma$ with variable working conditions. For example, Fig. 6 shows that protonic conduction is the dominant contribution in the yttrium-containing material at 800 °C, for a relatively wide range of oxygen partial pressures (10^{-15}–10^{-5} Pa). Unfortunately, this does not comprise the usual working conditions of potentiometric humidity sensors, which often operate at relatively high oxygen partial pressures. Note that the electron hole component $\sigma_p = \sigma_p^* (p_{O_2})^{1/4}$ is the largest conductivity contribution in air, and the upper

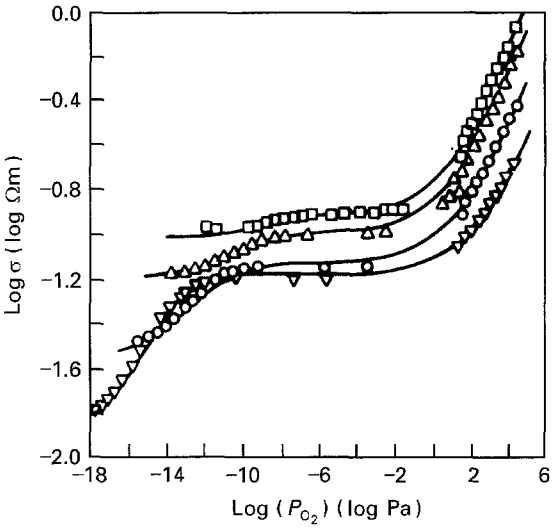

Figure 5 Electrical conductivity of $SrZr_{0.84}Y_{0.16}O_{2.92}$ versus the oxygen partial pressure at (▽) 800, (○) 900, (△) 1000 and (□) 1100 °C.

limit of the electrolytic domain (p_{O_2} where $t_p = \sigma_p/\sigma = 0.01$), corresponds to relatively reducing conditions (Table II). At 800 °C the upper limit of this electrolytic domain is $p_{O_2} \approx 8 \times 10^{-6}$ Pa.

Fig. 7 also shows that protons are the main ionic charge carriers in the SYZ sample for temperatures up to 900 °C, and for oxygen partial pressures in the range 10^{-15} – 1 Pa. Oxygen-ion conductivity prevails at higher temperatures. The decrease in protonic transport numbers in reducing conditions can be related to reduction of water vapour $2H_2O \rightarrow 2H_2 + O_2$, as shown earlier.

The experimental conductivity data for the lanthanum-containing material LSZ (Fig. 8) in the low oxygen partial pressure range are reasonably fitted by

$$\sigma = \sigma_{i1} + \sigma_n^*(p_{O_2})^{-1/4} \quad (7)$$

where the constant conductivity plateau ($\sigma \approx \sigma_{i1}$) is typical of ionic conduction. The relevant fitting parameters are the ionic conductivity, σ_{i1}, and the electronic conductivity, σ_n^*, when the oxygen partial pressure is 1 Pa. Note that the increase in conductivity for low oxygen partial pressures represents the onset of n-type conduction described by $\sigma_n = \sigma^*{}_n(pO_2)^{-1/4}$. The values are shown in Table I and were used to evaluate the lower limit of the electrolytic region ($\sigma_n/\sigma = 0.01$), shown in Table II.

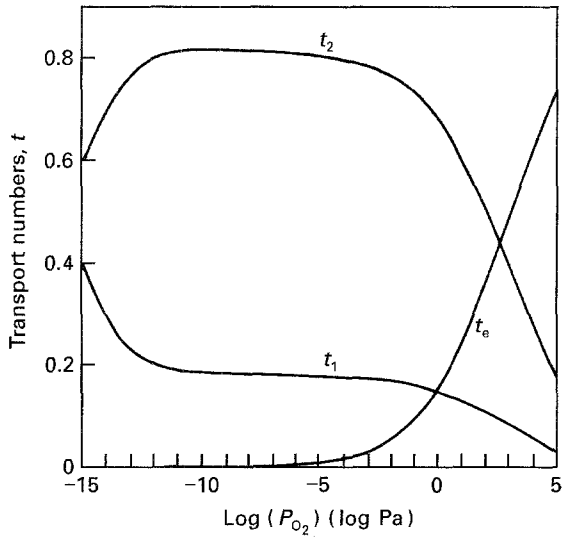

Figure 6 Predictions of the effects of oxygen partial pressure on the electronic, t_e, oxygen-ion, t_1, and protonic t_2, transport numbers in $SrZr_{0.84}Y_{0.16}O_{2.92}$ at 800 °C.

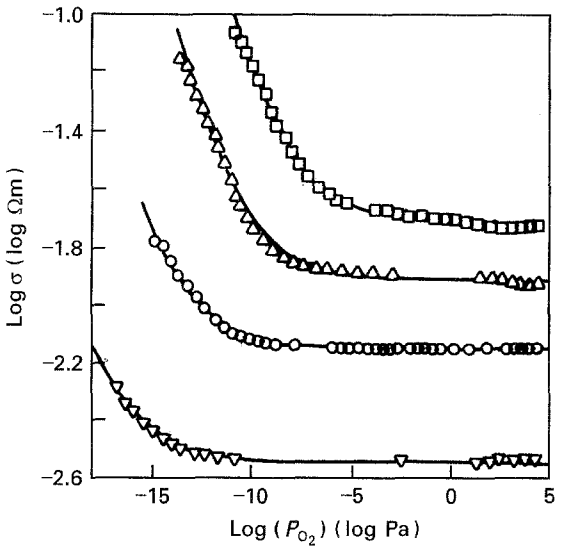

Figure 8 Electrical conductivity of $Sr_{0.95}La_{0.05}ZrO_{3.025}$ versus the oxygen partial pressure at (▽) 800, (○) 900, (△) 1000 and (□) 1100 °C.

TABLE II Upper or lower limits of the electrolytic domains of $SrZrO_3$ (SZ), $SrZr_{0.84}Y_{0.16}O_{2.92}$ (SYZ) and $Sr_{0.95}La_{0.05}ZrO_{3.025}$ (LSZ)

Temperature	Limits of electrolytic domains (Pa)		
(°C)	Upper SZ	Upper SYZ	Lower LSZ
800	–	8×10^{-6}	5×10^{-10}
900	7×10^{-6}	8×10^{-7}	4×10^{-7}
1000	10^{-7}	3×10^{-7}	1.3×10^{-3}
1100	9×10^{-9}	2×10^{-7}	0.2

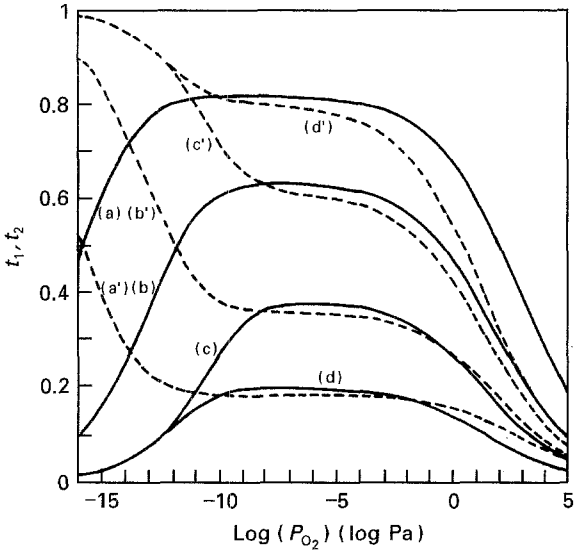

Figure 7 Predictions of the effects of oxygen partial pressure and temperature on ionic transport numbers in $SrZr_{0.84}Y_{0.16}O_{2.92}$. (—) The protonic transport numbers at (a) 800, (b) 900, (c) 1000, and (d) 1100 °C from top to bottom, and (- - -) the corresponding oxygen-ion transport numbers (a'–d') are shown.

Fig. 8 also suggests that lanthanum for strontium substitution suppresses the p-type contribution. Therefore, the dependence of conductivity on the oxygen partial pressure confirms that the dominant electronic and ionic charge carriers can be different for the lanthanum containing and yttrium-containing materials.

The explanation proposed by Labrincha *et al.* [26] for the effects of lanthanum for strontium substitution on the transport properties was based on the following reaction

$$La_2O_3 + 2ZrO_2 + V_O^{\cdot\cdot} \xrightarrow{SrZrO_3} 2La_{Sr}^{\cdot} + 2Zr_{Zr} + 7O_O \quad (8)$$

Combination with Equations 1 and 2 is consistent with vanishing electron hole and protonic conductivities. In addition, the onset of the n-type contribution in reducing conditions could also be accounted for by the following equilibrium

$$0 \rightleftharpoons e' + h^{\cdot} \quad (9)$$

According to Equation 9, n-type charge carriers are formed when the concentration of electron holes vanishes.

The increase in ionic conductivity relative to undoped $SrZrO_3$ represents an objection to the mechanism proposed for the lanthanum-containing material. Actually, the data for the SZ and SYZ materials are probably underestimated because these samples were quite porous. This was not the case for the lanthanum-containing samples, which were about 97% dense. Differences in density thus account partly for differences in the values of conductivity measured for porous SZ and dense LSZ samples. Nevertheless, the differences in ionic conductivity between the SZ and LSZ materials are probably higher than expected for the effect of density; this will be further discussed in Section 3.4.

3.3 Temperature dependence

The conductivity data in air were evaluated by impedance spectroscopy and were plotted in Fig. 3 as

$$\sigma T = \sigma_o \exp[-E_a/(RT)] \quad (10)$$

where E_a is the activation energy; this is a typical Arrhenius dependence expected for ionic conductors. The values of E_a are about 136, 59 and 116 kJ mol^{-1} for compositions SZ, SYZ and LSZ, respectively. The activation energy of the yttrium-containing composition (SYZ) is within the typical range for proton-conducting perovskites. However, the dependence of σ on the oxygen partial pressure shows that the electronic conductivity contribution in air might exceed the protonic contribution.

The temperature dependence of electronic and ionic conduction in undoped (SZ), lanthanum-containing (LSZ), and yttrium-containing (SYZ) materials was also computed from the fitting parameters shown in Table I. Figs 9 and 10 confirm that the transport properties of those materials are significantly different from each other. The activation energies, E_{ai}, for ionic conduction in air (Table III) were evaluated on assuming that the sum of both ionic contributions, $\sigma_i = \sigma_{i1} + \sigma_{i2}(1 + p_{H_2}/p_{H_2O})^{-1/2}$, varies as described by Equation 10. Note that the activation energies for ionic conduction in the undoped and yttrium-containing materials (Table III) are much smaller than expected for oxygen-ion conduction, even in relatively open oxide structures such as pyrochlores [33]. The values of activation energies for the SZ and SYZ materials are relatively close to the activation energy (≈ 43 kJ mol^{-1}) reported for protonic conduction in $SrZr_{0.95}Y_{0.05}O_{3-\delta}$ below about 500 °C [6]. The activation energy evaluated for the oxygen-ion contribution, σ_{i1}, in the yttrium-containing composition (97 kJ mol^{-1}) is also close to typical values found for oxygen-ion conductors.

The activation energy for ionic conduction in the lanthanum containing LSZ material (88 kJ mol^{-1}) is about 10% less than for σ_{i1} in the yttrium-containing material; this also suggests oxygen-ion conduction in LSZ.

The activation energies for either p-type or n-type conduction were evaluated from the temperature dependence of electronic contributions at $p_{O_2} = 1$ Pa (σ_p^*, or σ_n^*); this is shown in Fig. 10 on assuming the dependence

$$\sigma_e^* = \sigma_{eo} \exp[-E_{ae}/(RT)] \quad (11)$$

where $\sigma_e^* = \sigma_p^*$ for the undoped and yttrium-containing materials and $\sigma_e^* = \sigma_n^*$ for the lanthanum-containing material.

The activation energy evaluated for n-type conductivity in the lanthanum-containing material ($E_{an} = 285$ kJ mol^{-1}) is much higher than for p-type conduction in the undoped and yttrium-containing materials. In addition, the value computed for p-type conduction in the undoped sample SZ ($E_{ap} = 158$ kJ mol^{-1}) is much higher than the value $E_{ap} = 62$ kJ mol^{-1} obtained for the yttrium-containing material SYZ. This difference between the values of E_{ap} for SZ and SYZ suggests a change from intrinsic to extrinsic behaviour.

The activation energy for the conductivity of lanthanum-containing LSZ in air, E_a, is only moderately different from the activation energy evaluated for the ionic conductivity, E_{ai}, and is very different from E_{an}; this shows that the behaviour in air is determined mostly by ionic transport. The differences between E_a and E_{ai} are probably related to the grain-boundary contribution which is mostly effective for temperatures lower than about 800 °C (see Figs 1 and 2).

A comparison between the values of E_a evaluated for the conductivity data in air, and the activation energies obtained for the ionic, E_{ai}, and electronic,

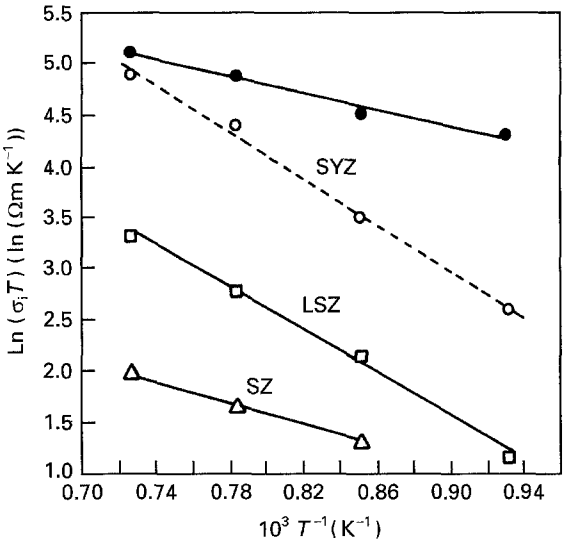

Figure 9 Arrhenius plots for the ionic conductivity of $SrZrO_3$ (SZ), $SrZr_{0.84}Y_{0.16}O_{2.92}$ (SYZ) and $Sr_{0.95}La_{0.05}ZrO_{3.025}$ (LSZ). (– – –) The oxygen-ion contribution in SYZ.

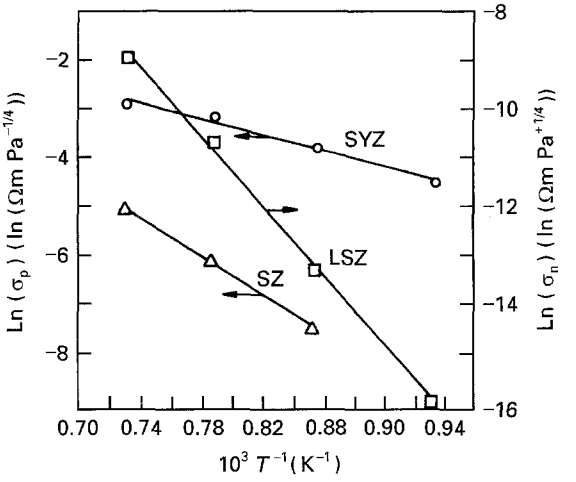

Figure 10 Arrhenius plots for the electronic conductivity of $SrZrO_3$ (SZ), $SrZr_{0.84}Y_{0.16}O_{2.92}$ (SYZ) and $Sr_{0.95}La_{0.05}ZrO_{3.025}$ (LSZ) at the reference oxygen partial pressure of 1 Pa.

TABLE III Activation energies for ionic and electronic conductivities in materials with compositions $SrZrO_3$ (SZ), $SrZr_{0.84}Y_{0.16}O_{2.92}$ (SYZ) and $Sr_{0.95}La_{0.05}ZrO_{3.025}$ (LSZ)

Composition	Activation energies (kJ mol^{-1})			
	E_a	E_{ai}	E_{ap}	E_{an}
SZ	136	45	158	–
SYZ	59	36 (97)	62	–
LSZ	116	88	–	285

E_{ap} and E_{an}, contributions shows that the behaviour of the undoped (SZ) and yttrium-containing (SYZ) materials in air is mostly determined by their electronic contributions. This observation is consistent with the relatively high electron hole transport numbers in air (Fig. 6). In addition, the activation energy computed for the conductivity of SYZ in air, E_a, is quite different from the activation energy evaluated for oxygen-ion conduction, and only slightly higher than expected for the protonic contribution. Therefore, the protonic transport number must increase with decreasing temperature, and the oxygen-ion transport number decreases.

However, the value of $E_a = 59\ kJ\ mol^{-1}$ computed by fitting the conductivity of composition SYZ in air, refers to temperatures down to about 400 °C, and is close to the value evaluated for the electron hole contribution ($E_{ap} = 62\ kJ\ mol^{-1}$). Significant electron hole transport numbers are thus expected even at temperatures lower than 500 °C, which represents a serious limitation of these proton-conducting materials.

3.4. Concluding remarks on ionic transport in $Sr_{1-x}La_xZrO_{3+\alpha}$

The interpretation of experimental data leads to some doubts about the major ionic charge carried in $Sr_{0.95}La_{0.05}ZrO_{3.025}$ (LSZ). In fact, the activation energy ($E_{ai} = 88\ kJ\ mol^{-1}$) suggests oxygen-ion conduction. In addition, the ionic conductivity of LSZ at $T \geq 800$ °C is higher than for the undoped composition, which contradicts the expected effects of lanthanum for strontium substitution on the proposed defect chemistry (Equation 8).

An alternative formulation for the defect chemistry involving oxygen ions in interstitial positions is unlikely for the close-packed perovskite structure. Lanthanum for strontium substitution causes a decrease in the lattice parameters for LSZ, which suggests the formation of cation vacancies,, as previously proposed by other authors [4]. In addition, lanthanum for strontium substitution is very effective in enhancing the sinterability of $SrZrO_3$-based materials, which might be attributed to promoting cationic transport at high temperatures. However, cationic transport is unlikely to contribute to the electrical conductivity, because the differences between the a.c. and d.c. conductivity measurements in air are within about 5% only. Note that this error can be attributed to the selection of a standard frequency (10^4 Hz) for a.c. measurements. A significant polarization effect should be observed if a cationic species were the major charge carrier.

Finally, disorder in the A-site positions of the ABO_3 perovskite might contribute to enhance the mobility of oxygen ions. For example, A-site vacancies might assist atomic rearrangements required for ionic conduction. Atomic rearrangements might also be effected by shifting a fraction of La^{3+} ions between the A and B sites, as suggested by Eror and Balachandran [34] for the distribution of lanthanum in $SrTiO_3$-based materials.

4. Conclusion

Conductivity measurements versus the oxygen partial pressure can be used to evaluate the transport properties of potential protonic conductors. $SrZr_{1-x}Y_xO_{3-\alpha}$ materials are mixed ionic and p-type conductors in air. Conductivity data suggest that the ionic conduction of undoped or yttrium-containing materials gradually changes from protonic to oxygen-ion conduction with increasing temperature. On the contrary, the protonic conduction is suppressed in the lanthanum-containing material. The interpretation of ionic conduction in this composition was somewhat inconclusive.

Both p-type conduction and ionic transport are enhanced by yttrium for zirconium substitution. The onset of n-type electronic conduction was observed for lanthanum-doped $SrZrO_3$ in reducing conditions; this corresponds to about 10^{-10} Pa at 1000 °C. Changes in composition may thus be used to design the materials properties.

Acknowledgement

This work was sponsored by Junta Nacional de Investigação Científica e Technológica (JNICT), Portugal.

References

1. A. M. ANTHONY and M. FOEX, in "Proceedings of symposium on magnetic hydrodynamic electrical power", Vol. 3, (National Agency for International Publication Inc., New York, 1966) p. 265
2. T. NOGUCHI, T. OKUBO and O. YONEMOCHI, *J. Am. Ceram. Soc.* **52** (1969) 179.
3. H. STETSON and B. SCHWARTZ, *ibid.* **44** (1961) 420.
4. N. SURIYAYOTHIN and N.G. EROR, *J. Mater. Sci.* **19** (1984) 2775.
5. M. ZBOROWSKA, M. GRYLICKI and J. ZBOROWSKI, *Ceram. Int.* **6** (1980) 99.
6. S. SHIN, H. H. HUANG, M. ISHIGAME and H. IWAHARA, *et al., Solid State Ionics* **40/ 41** (1990) 910.
7. H. H. HUANG, M. ISHIGAME and S. SHIN, *ibid.* **47** (1991) 251.
8. T. HIBINO, K. MUZUTANI, T. YAJIMA and H. IWAHARA, *ibid.* **57** (1992) 303.
9. H. IWAHARA, T. YAJIMA, T. HIBINO, K. OZAKI, H. SUZUKI, *ibid.* **61** (1993) 65.
10. H. IWAHARA, T. ESAKA, H. UCHIDA and N. MAEDA, *ibid.* **3/4** (1981) 359.
11. T. SCHERBAN and A. S. NOWICK, *ibid.* **35** (1989) 189.
12. H. IWAHARA, *ibid.* **52** (1992) 99.
13. N. BONANOS, *ibid.* **53–56** (1992) 967.
14. T. YAJIMA, H. IWAHARA and H. UCHIDA, *ibid.* **47** (1991) 117.
15. J. F. LIU and A. S. NOWICK, *ibid.* **50** (1992) 131.
16. A. MITSUI, M. MIYAYAMA and H. YANAGIDA, *ibid.* **22** (1987) 213.
17. H. IWAHARA, H. UCHIDA, K. OGAKI and H. NAGATO, *J. Electrochem. Soc.* **138** (1991) 295.
18. T. YAJIMA, H. KAZEOKA, T. YOGA and H. IWAHARA, *Solid State Ionics* **47** (1991) 271.
19. R. L. COOK, J. J. OSBORNE, J. H. WHITE, R. C. MACDUFF and A.F. SAMMELLS, *J. Electrochem. Soc.* **139** (1992) L19.
20. M. J. SCHOLTEN, J. SCHOONMAN J. C. VAN MILTENBURG and H. A. J. OONK, *Solid State Ionics* **61** (1993) 83.
21. H. IWAHARA, H. UCHIDA and S. TANAKA, *ibid.* **9/10** (1983) 1024.
22. H. UCHIDA, N. MAEDA and H. IWAHARA, *ibid.* **11** (1983) 117.

23. H.H. HUANG, M. ISHIGAME and S. SHIN, *ibid.* **47** (1991) 251.
24. S. HAMAKAWA, T. HIBINO and H. IWAHARA, *J. Electrochem. Soc.* **140** (1993) 459.
25. N. TANIGUCHI, K. HATOH, J. NIIKURA and T. GAMO, *Solid State Ionics* **53–56** (1992) 998.
26. J. A. LABRINCHA, J. R. FRADE and F. M. B. MARQUES, *ibid.* **61** (1993) 71.
27. Y. M. KAIKOV and E. K. SSHALKOVA, *J. Solid. State Chem.* **97** (1992) 224.
28. T. YAJIMA and H. IWAHARA, *Solid State Ionics* **50** (1992) 281.
29. F. M. B. MARQUES and G. P. WIRTZ, *J. Am. Ceram. Soc.* **74** (1991) 598.
30. T. NORBY, O. DYRLIE and P. KOFSTAD, *ibid.* **75** (1992) 1176.
31. T. NORBY and P. KOFSTAD, *ibid.* **67** (1984) 786.
32. *Idem, ibid.* **69** (1986) 784.
33. M. P. VAN DIJK, K. J. DE VRIES and A. J. BURGGRAAF, *Solid State Ionics* **9/10** (1983) 913.
34. N. G. EROR and U. BALACHANDRAN, *J. Solid State Chem.* **40** (1981) 85.

Received 16 June 1994
and accepted 20 January 1995